Techno-economic assessment of two novel feeding systems for a dry-feed gasifier in an IGCC plant with Pd-membranes for CO_2 capture

Matteo Gazzani [a,*], Davide M. Turi [a], Ahmed F. Ghoniem [b], Ennio Macchi [a], Giampaolo Manzolini [a]

[a] *Politecnico di Milano, Dipartimento di Energia, Via Lambruschini 4, 20156 Milano, Italy*[1]
[b] *Massachusetts Institute of Technology, Department of Mechanical Engineering, 77 Massachusetts Avenue, Cambridge, MA, USA*[2]

Received 18 November 2013
Received in revised form 7 March 2014
Accepted 21 March 2014
Available online 25 April 2014

1. Introduction

The rise of carbon dioxide concentration in the atmosphere and its potential negative impact on the climate has prompted research towards environmentally friendly electricity production technologies. Among existing technologies for low CO_2 electricity production, e.g., solar, wind, biomass, geothermal, and nuclear, fossil-fuel based plants with CO_2 capture are the most scalable in the mid-term (DOE, 2007; IEA, 2008). Three CO_2 capture technologies in power plants have been identified: post-combustion, oxy-combustion and pre-combustion capture.

Post-combustion capture relies on separating CO_2 from the flue gases via chemical or physical absorption. For this purpose, amine scrubbing is the state-of-the-art technology (Amrollahi et al., 2011; Rao and Rubin, 2002; Wang et al., 2011). Advanced post-combustion capture technologies with better performance have been proposed and are under investigation (Chiesa et al., 2011; Riberiro et al., 2012; Valenti et al., 2012).

Oxy-combustion capture is based on fuel combustion in an oxygen environment (for a comprehensive review, see Chen et al., 2012). Many advances have been made in oxygen production and its integration with the combustion process to improve the overall efficiency of the plant (Hong et al., 2010). Depending on the fuel and the plant layout further gas purification steps may be necessary to separate inert gases and other pollutants from the CO_2 stream before storage (Hong et al., 2010; White et al., 2010). The efficiency and economic impact of these additional conditioning steps must be considered while evaluating the technology.

In the pre-combustion decarbonisation concept, the carbon-bounded energy is first transferred from the primary fuel to hydrogen; hydrogen can then be burned in a combined cycle, producing power without CO_2 emission. In coal-based plants, as assumed in this work, the pre-combustion technology fits perfectly into Integrated Gasification Combined Cycles (IGCC). IGCC

* Corresponding author. Current address: ETH Zurich, Institute of Process Engineering, CH-8092 Zurich, Switzerland. Tel.: +41 446322514; fax: +41 446321141.
E-mail addresses: matteo.gazzani@mail.polimi.it, gazzanim@ethz.ch (M. Gazzani).

[1] www.gecos.polimi.it.
[2] http://web.mit.edu/rgd/www/.

Nomenclature and acronyms

AGR	acid gas removal
CCR	carbon capture ratio (%)
CCS	carbon capture and storage
CGE	cold gas efficiency
COT	combustor outlet temperature (°C)
E	CO_2 emission rate (kg_{CO2}/kWh_{el})
GT	gas turbine
HPHT	high pressure high temperature
HR	heat rate (kJ_{LHV}/kWh_{el})
HRF	hydrogen recovery factor
HRSC	heat recovery steam cycle
HRSG	heat recovery steam generator
IGCC	integrated gasifier combined cycle
LP	low pressure
PF	post firing
SEWGS	sorption enhanced water gas shift
SH	super heating
SPECCA	specific primary energy consumption for CO_2 avoided (MJ_{LHV}/kg_{CO2})
STFT	stoichiometric flame temperature (K)
TIT	turbine inlet temperature (total temperature ahead of the GT first rotor) (°C)
TIT_{iso}	GT inlet temperature (defined according to ISO standard) (°C)
TOT	GT outlet temperature (°C)
WGS	water gas shift
WGSR	water gas shift reactor
η	efficiency (%)

Subscripts

el	electrical
REF	reference

consists of a high pressure reactor which converts coal into syngas; the gasification pressure depends on the technology: the Shell–Prenflo dry-fed gasifier works near 40 bar (Franco et al., 2011, 2010; Gazzani et al., 2013b), while the GE's slurry fed technol-ogy at 70 bar (DOE/NETL-2011/1498, 2011). The produced syngas can then be utilized in a combined cycle. Available technologies for CO_2 capture in IGCC plants are commercial Acid-Gas Removal (AGR) systems such as Rectisol™, Selexol® or Sulfinol® (DOE/NETL-2011/1498, 2011; Franco et al., 2010). The AGR is composed of two steps, the first dedicated to sulphur removal while the second to CO_2 separation. Some of the concerns regarding these technologies include the significant efficiency penalty and the cost of the extra equipment.

Currently, research in carbon capture from fossil-based power plants is focused on advanced CO_2 separation processes that reduce both the economic and efficiency penalties (current efficiency penalty far exceeds that the corresponding Second law minimum separation energy). Some of the innovative technologies being explored are low temperature sorbents (Casas et al., 2012; Schell et al., 2013), medium temperature sorbents integrated in the water–gas-shift reactors, also called SEWGS (Dijk et al., 2011; Manzolini et al., 2013) and calcium looping (Martinez et al., 2013). Among other promising technologies under investigation are gas separation membranes (Anantharaman and Bolland, 2011; Bredesen et al., 2004; Chiesa et al., 2007; Hong et al., 2012; Scholes et al., 2010). This is because of their simplicity, low separation energy penalty, ease of integration with the power plant and, potentially, low cost.

In our previous work, the integration of hydrogen-selective membranes developed in the CACHET-II project for a Shell-gasifier based IGCC plants was investigated (Gazzani et al., 2014b). The main findings of that work are:

- Membranes modules are considered instead of membrane reactors because of techno-economics reasons and plant operation concerns.
- The membrane separation section constitutes a significant share of the overall costs.
- To limit the membrane surface area (i.e., costs) not all the hydrogen in the syngas is separated at high pressure for use as fuel in the gas turbine. Instead a small amount of the available hydrogen in the syngas (about 10%) must be separated at low pressure for post-fire in the HRSG.
- As consequence of N_2 presence in the syngas related to fuel charging, a cryogenic separation unit is necessary to achieve the required CO_2 purity for storage.
- Pd-based membranes with sulfur tolerance developed in CACHET-II project (Peters et al., 2012; Song and Forsyth, 2013; Van Berkel et al., 2013) are not yet economically competitive as compared to pure Pd membranes.

As shown in Gazzani et al. (2014b) and reported in Fig. 1, using of different gases for coal feeding impacts the rest of the plant in significant ways. In the previous work, the conventional solution in which nitrogen is used as coal pressurizer, carrier and candle filters cleaner was investigated. This work, on the other hand, focuses on the application of palladium membranes in IGCC plants with CO_2 as the principal gas for coal feeding (Guo et al., 2012). Some of the primary advantages of adopting CO_2 as a fuel carrier and backflushing include the higher CO_2 purity at the outlet of the membrane reactor. With a conventional gasifier, the CO_2 purity in the retentate at the membrane outlet is quite low because of the nitrogen content.
In this case, an extra purification step is necessary to upgrade CO_2 purity above the 96% threshold (Franco et al., 2011, 2010). In the CO_2 feeding case, the retentate can be combusted in oxygen hence by utilizing the energy of its hydrogen content while maintaining high CO_2 purity. Therefore, this configuration simplifies the plant layout because the cryogenic system is replaced by an oxy-combustor (we note that the Air Separation Unit (ASU) already exists in the IGCC plant).

2. Using CO_2 as coal carrier: gasifier modelling and feeding technology assessment

In an entrained flow gasifier, the syngas composition is mainly affected by: (i) the type of coal used as a feedstock, (ii) the reactor thermodynamic conditions and (iii) the coal feeding system. While the first and the second point strongly affect the entire gasification process, the influence of the coal carrier is not always straightforward but depends on several system characteristics (e.g., dry or wet feed) and coal carrier reactivity. As far as a dry fed gasifier is concerned (e.g., Shell, Siemens, MHI, etc.) the coal feeding uses part of the nitrogen produced in the ASU. Being an inert gas, nitrogen does not affect the process except for its sensible energy. On the other hand, there are specific cases where CO_2 is the preferred feeding gas. Contrary to nitrogen, CO_2 cannot be considered as inert; it affects the kinetics of many reactions (Botero et al., 2013, 2012). Furthermore, and depending on the syngas end-use, CO_2 can be adopted to match the required H_2/CO ratio or to limit the amount of inert gases in the produced syngas (usually nitrogen and argon).

Given the heterogeneity of the coal chemical structure and the three phase conditions inside the reactor, coal gasification is a

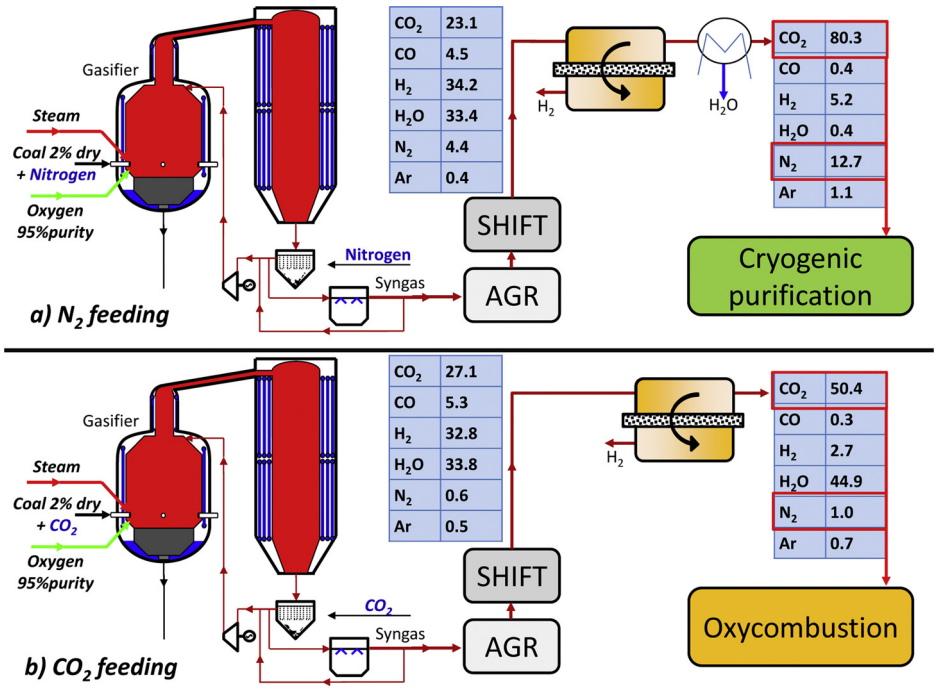

Fig. 1. A schematic diagram of the gasification and hydrogen separation section: on the left the gasifier and syngas cooler followed by the acid-gas removal, the water gas shift reactor and the membrane modules for H_2 recovery. Depending on the feed type, two layouts are shown: (a) gasifier with N_2 as coal carrier and (b) gasifier with CO_2 as coal carrier. Numbers refer to HRF = 95%.

complex process. Extensive progress has been made in modelling coal kinetics and in CFD modelling of coal gasification (Abani and Ghoniem, 2013; Kumar and Ghoniem, 2012). Nevertheless, the reactor design and operation have long relied on practical experience rather than on theoretical modelling. With regard to the Shell gasifier, the syngas composition after the scrubber is known when coal is pressurized and fed with nitrogen (Gazzani et al., 2013a). On the other hand, given that use of CO_2 as coal carrier has only been proposed recently, no experimental data are available. In this study, the kinetic model presented in Gazzani et al. (2013b) has been used to predict the syngas composition along the entire process. The amount of gas needed for candle filters backflushing and coal feeding have been updated according to the most recent data (Prins, 2012).

When CO_2 is adopted as a coal carrier, there are two main strategies to control the gasification process: (i) maintain the same amount of oxidant while calculating the new gasifier outlet temperature; or (ii) increase the amount of oxygen for the same (or slightly higher) gasifier outlet temperature. From a simulation point of view, the first option is suitable when using a kinetic model (ROM or CFD) while the second one fits well the equilibrium approach, where the equilibrium temperature must be set in order to fairly reproduce a reference syngas composition. Consistent with the results shown in Gazzani et al. (2013b), the first method was adopted in this work. In both cases the amount of CO_2 required is defined by keeping the overall volumetric flow at the lockhopper system constant. This is therefore dependent on the nitrogen volumetric flow at the given temperature and pressure and the lockhopper technology considered.

The dry feeding system is a simple and fairly reliable technology, widely applied for feeding solids in pressurized reactors. While the associated energy penalty is relatively low, the technology is limited to relatively low gasifier pressure. On the other hand, the operation of the lockhopper system becomes critical when CO_2 is adopted as the feeding gas and CCS is considered. This is because a significant amount of gas could be vented unintentionally during the feeding process in its basic configuration, and CO_2 emission would increase significantly affecting the efficiency of the capture process. In order to cope with this drawback, different improvements should be adopted depending on the process layout. Fig. 2 reports three different configurations for a CO_2 gas feeding system used with a dry gasifier:

- Conventional, nitrogen-based layout: part of the available nitrogen from the ASU is compressed and utilized to pressurize three different reactors: the storage bin, the lockhopper and the feeding vessel, while another part is directly sent to the conveying tube to transport the pressurized coal inside the gasifier. Overall, about 0.44 kg of nitrogen is required for each kg of coal.
- Advanced, CO_2-based system: in this case, the layout is similar to the nitrogen case except for the feed gas, now CO_2, and the amount of gas needed (while it is almost the same volumetric flow, the mass flow rate is different). Various modifications must be introduced in order to recover the CO_2 to be utilized for the vessel pressurization. The recovered amount depends on the technology constraints and the cost of the system. No additional compressors are required as high pressure CO_2 is recovered from the liquefaction train after the separation.
- State-of-the-art nitrogen + CO_2 system: according to Schinignitz and Tietze (2008) a mixed nitrogen + CO_2 layout can be adopted to reduce the amount of nitrogen fed to the gasifier. Given the process configuration, only part of the CO_2 is vented together with nitrogen from the lockhopper reactor.

In this work, two different scenarios are considered: (i) the CO_2 based system with no venting and (ii) the CO_2 based system with partial recovery of the vented gas (90%). As such, in the following performance tables, two different values of Specific Primary Energy for CO_2 Consumption (SPECCA) are provided. The

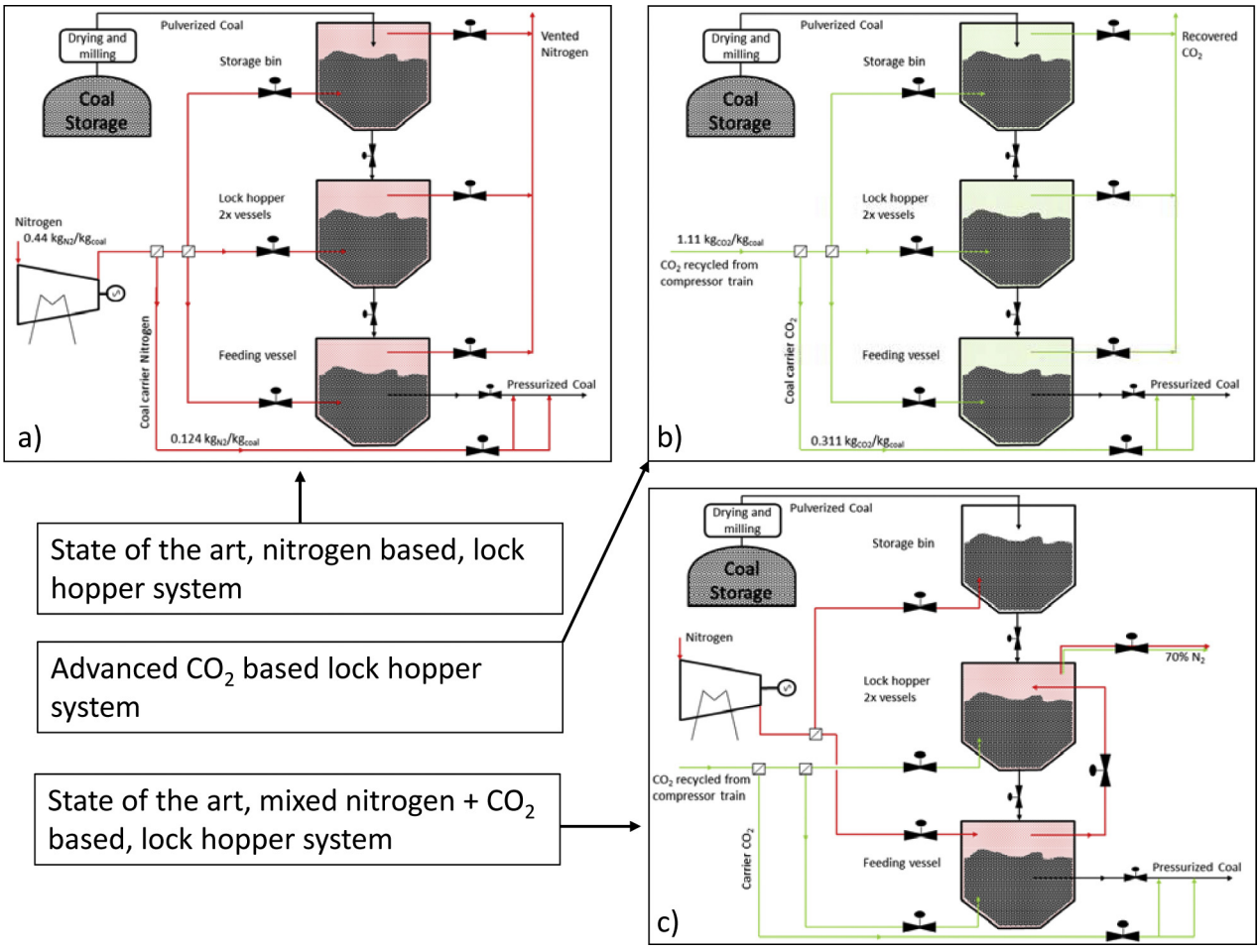

Fig. 2. Representation of the lockhopper feeding system: once coal is dried and milled to the desired size it is sent to the lockhopper system, which is generally made of two or three vessels. Depending on the pressurizer and carrier gas different layouts are adopted: (a) nitrogen-based lock hopper system, (b) advanced-system with CO_2 feeding, (c) commercial, mixed CO_2 and nitrogen system as reported in Schinignitz and Tietze (2008).

mixed nitrogen + CO_2 shown in Fig. 2 has not been considered due to the lack of quantitative data.

As far as the Shell gasification process is concerned, an inert gas is adopted to pressurize and feed the coal into the gasifier but also for continuous cleaning of the candle filters (also named as High Pressure High Temperature HPHT filters) after the syngas cooler. Depending on the final use of the syngas, different combinations of nitrogen and CO_2 can be utilized to improve the plant performance and/or the economics. In case of power production, nitrogen is employed both in the lockhopper and in the HPHT filters. On the other hand, when the syngas must have a specific CO to H_2 ratio, in the case of chemicals production or for liquid fuel synthesis, CO_2 is generally chosen as the feed gas. An hybrid configurations with use of nitrogen together with CO_2 can also be adopted.

Consistently, two different layouts are proposed in this work: the first, named *CO_2 feeding*, features the use of CO_2 as fuel carrier as well as CO_2 for backflushing the HPHT filters. In the second, named *hybrid*, CO_2 is adopted exclusively for backflushing the HPHT filters while coal is fed with N_2 based system. In both configurations the required amount of high purity CO_2 is taken from the total volume separated inside the plant and intended for the storage. Accordingly, no significant extra components (as compared to the plant with nitrogen feeding) are required. Finally, it is worth noting that CO_2 is supercritical at the pressure required by the HPHT filters and in order to keep the same density as nitrogen and thus prevent filter malfunctioning the CO_2 stream should be heated to about 200 °C.

Fig. 3 shows detailed layouts of the reference Shell gasification process. The ASU is on the left-hand side of the diagram together with the intercooled compressors. The gasifier is on the right-hand side together with the syngas cooler and other equipment. Table 1 reports the temperature, pressure, mass flow and compositions at two important sections along the gasification process: (i) the gasifier reactor outlet and (ii) the scrubber outlet. All the gasifier configurations are reported, i.e., the nitrogen based, the CO_2 based and the hybrid layout. The reported data were obtained using the kinetics-based reduced order model presented and validated in Gazzani et al. (2013b).

3. Membrane configuration

Most of the work done on the use of membranes in IGCC plants proposed the adoption of membrane reactors so that the primary fuel conversion, hydrogen generation and separation are carried out in the same reactor. Besides equipment savings, membrane reactors can increase the amount of hydrogen separated because of the continuous product separation which drives the reaction towards the product side. Another concept consists of a non-integrated sequential series of alternating membrane modules and adiabatic reactors membrane separator modules (Song and Forsyth, 2013; Van Berkel et al., 2013). The adoption of membrane

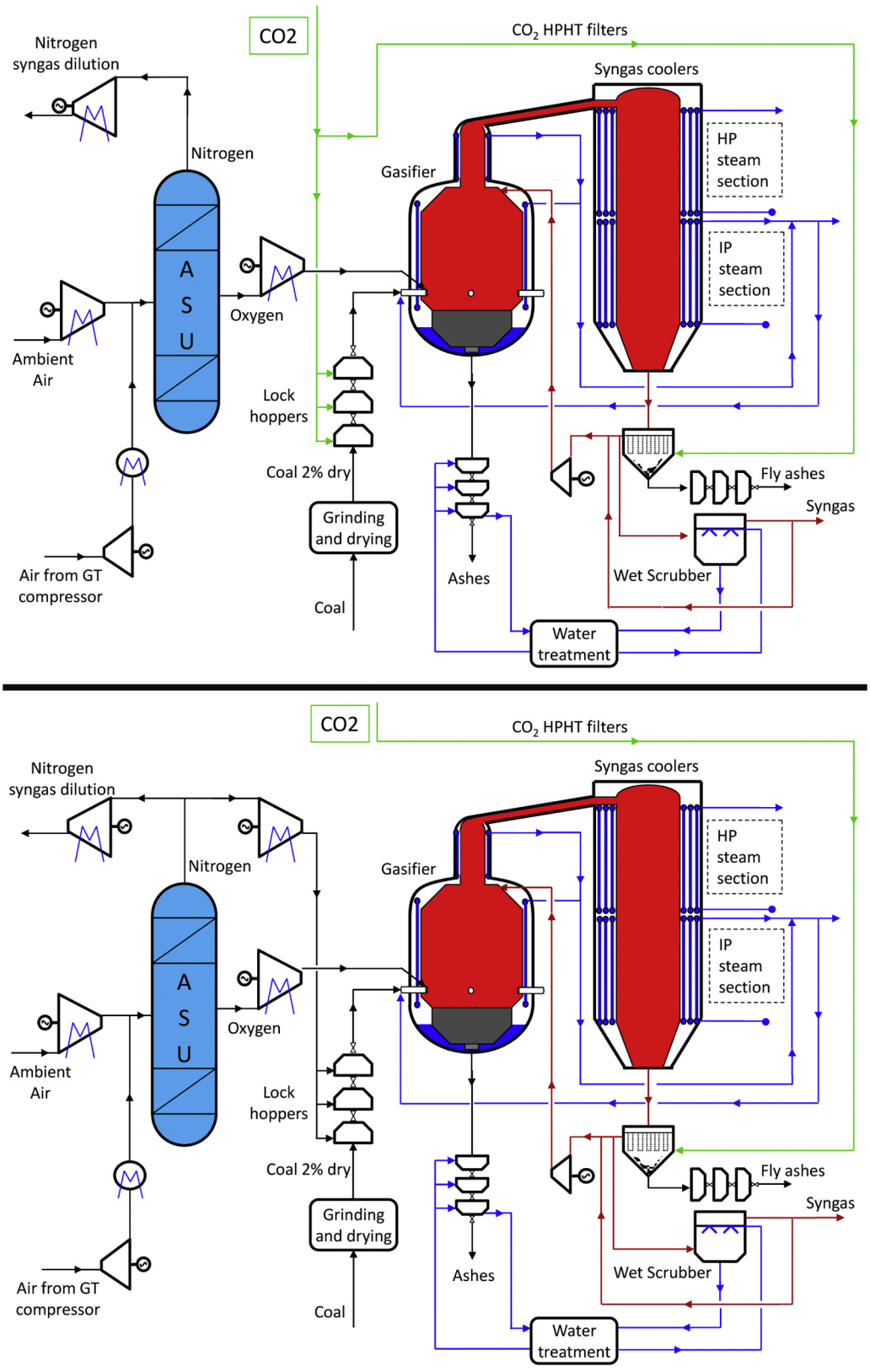

Fig. 3. The gasifier island layout (comprising: ASU and its compressors, gasifier reactor, syngas cooler, lockhopper system, candle filters, wet scrubber and water treatment) for the cases in which: (a) CO_2 (in green) is adopted both as fuel carrier and candle filters purge gas, and (b) nitrogen is used to charge the coal while CO_2 purifies the candle filters.

Table 1
Temperature, pressure, mass flow, composition and cold gas efficiency for the gas phase at the most relevant points of the gasification process. Values are reported for three different layouts of the feeding/HPHT filter cleaning: nitrogen base case, CO_2 feeding and hybrid case.

	T (°C)	p (bar)	G (kg/s)	Chemical species molar concentration (% mol)								CGE (%)
				CO	H_2	CO_2	H_2O	CH_4	H_2S	N_2	Ar	
Nitrogen feeding gasifier												
Gasifier exit	1588	43.8	81.7	62.28	25.93	1.05	1.78	–	0.17	7.87	0.92	83.0
Scrubber exit	160.6	41.1	95.5	50.59	23.41	2.58	14.12	–	0.16	8.37	0.77	82.6
CO_2 feeding gasifier												
Gasifier exit	1505	43.8	99.3	65.55	21.86	4.49	5.56	–	0.17	1.35	1.02	84.4
Scrubber exit	164	41.1	121.5	53.35	18.76	8.62	16.98	–	0.16	1.2	0.92	83.4
Hybrid feeding gasifier												
Gasifier exit	1588	43.8	81.8	62.28	25.93	1.05	1.78	–	0.17	7.87	0.92	83.0
Scrubber exit	164	41.1	101.9	49.48	22.93	6.68	13.49	–	0.15	6.51	0.77	82.6

Values have been obtained with the kinetic model reported in Gazzani et al. (2013b)

separator modules simplifies the substitution of the membranes thanks to the absence of the catalyst within the membranes. In addition, membrane separation modules do not suffer from the same feed side temperature gradients found in membrane reactor where the water-gas shift reaction is performed (the WGS is mildly exothermic). Multiple WGS reactors increase the CO conversion and consequently the amount of hydrogen that can be separated, usually named Hydrogen Recovery Factor (HRF). Given the typical conversion of a high temperature shift, one WGS reactor is sufficient for HRF lower than 90%, while additional reactor + membrane module stages are required for higher values (i.e., HRF >90%). Another advantage of this configuration is the higher feed velocity in the membrane modules which significantly reduces polarization con-centration losses. Previous work (Gazzani et al., 2014b) already outlined how polarization concentration can be detrimental for the hydrogen flux, hence a turbulent regime should be established inside the reactor. A turbulent regime with the membrane diameter and length considered in CACHET-II (1 in diameter and 6 m length) can be achieved only by adopting three membrane modules in series with adiabatic reactors in between.

A schematic of the hydrogen separation concept developed in CACHET-II and adopted in this work is shown in Fig. 4. It should be noted that there is a compressor upstream of the separation section and hydrogen is separated at two different pressures. The compressor is used because higher feed pressure increases the driving force for permeation, which hence reduces the required membrane surface area. A small amount of hydrogen (10%) is separated close to ambient pressure and is used for the heat recovery steam generator (HRSG) post-firing. Using part of the hydrogen to post-fire the HRSG, can be beneficial from the electric efficiency point of view thanks to the optimized heat transfer in the steam generator.[3] Moreover, it increases the permeation driving force in the very last part of the membrane area, which is usually the most critical, as the H_2 concentration decreases on the feed side. Cases with all the hydrogen separated at high pressure will also be presented for comparison.

4. Layout

The reference IGCC plants with and without capture have been taken from European Benchmark Task Force (EBTF) where Shell contributed the characterization of the gasification island (Franco et al., 2011, 2010). The overall plant, equilibrium-based, model was calibrated in order to provide the same syngas composition and auxiliaries consumption provided by the kinetics reduced-order model of the gasifier (Gazzani et al., 2013b). In all cases, due to the low membrane tolerance to sulfur (i.e., S concentration must be kept below 1 ppm in order to limit flux reduction), membranes were placed downstream the Rectisol®. In the following paragraph, the two different solutions introduced above are presented and explained in detail.

4.1. CO_2 feeding

The layout of the CO_2 feeding case, see Fig. 5, is the same as the reference IGCC of the Shell until the Acid Gas Removal (AGR). The only difference is in the stream used to feed the fuel and back-flush the filters. Advanced layouts were not considered in order to be consistent with the reference cases (Franco et al., 2010; Gazzani et al., 2013a). The gasification pressure is set at 44 bar, as indicated by Shell; this is a trade-off between efficiency, which benefit from a lower pressure, and the gasifier size. Coal is fed to the gasifier using CO_2 as carrier gas at 80 °C and 48 bar. The CO_2 stream is available at this pressure at the outlet of the CO_2 compressor. The power plant is sized on a combined cycle based on a single gas turbine. The gasification train generates syngas accordingly. The ASU for the gasifier oxygen production is in part integrated to the gas turbine compressor: the GT compressor supplies 50% of the air required by the ASU distillation column with an expander in between to recover part of the compression work. This configuration was proposed as reference from the EBTF. The by-product of the ASU, N_2, is used as a sweep gas in membrane modules in order to reduce the hydrogen partial pressure at the permeate side and hence lead to surface area reduction. Moreover, nitrogen is used as inert to limit NO_x formation by reducing the flame temperature. The hot syngas at the gasifier outlet is quenched to 900 °C by cold syn-gas recycling and then cooled down to 300 °C producing HP and IP steam. HP and IP steam are sent to the HRSG. Downstream, the syn-gas enters the cleaning section that consists of ceramic filters and a scrubber to remove the flyash, solids and soluble contaminants. After the scrubber, syngas is cooled from 170 °C down to ambient temperature producing hot water for the saturator. The ambient temperature is set by the AGR unit. H_2S and COS are removed in the AGR section by means of a Rectisol® which is based on chilled methanol (Korens et al., 2002). Separated H_2S is sent to the sulfur recovery unit. The syngas is then compressed up to 54 bar (cases with lower feed pressure are also evaluated) and saturated; additional steam is added to achieve a H_2/CO ratio equal to 2.0 at WGS inlet.

Additional steam comes from the IP steam generated in the gasification island and, if necessary, from the steam turbine at the high-pressure section outlet (usually named cold RH). The

[3] Combined cycles with additional steam introduced to the water drums can suffer from the lack of high temperature heat input from the gas turbine, penalizing the heat recovery efficiency. Post-firing can increase the temperature of the thermal power in the HRSG balancing the heat transfer with efficiency gains.

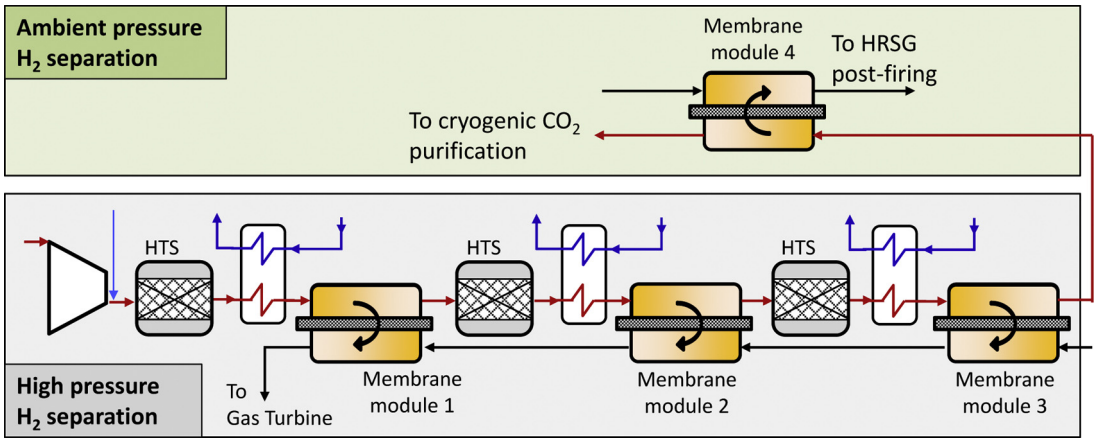

Fig. 4. A schematic diagram of the membrane separation concept adopted in CACHET-II: three membrane modules with compression of the feed stream. High Temperature Shift (HTS) reactors are place in before and in between the membrane separation units, as well as heat exchangers to cool the shifted gas. The last membrane unit operates at atmospheric pressure and the hydrogen produced is sent to the HRSG post-firing combustor.

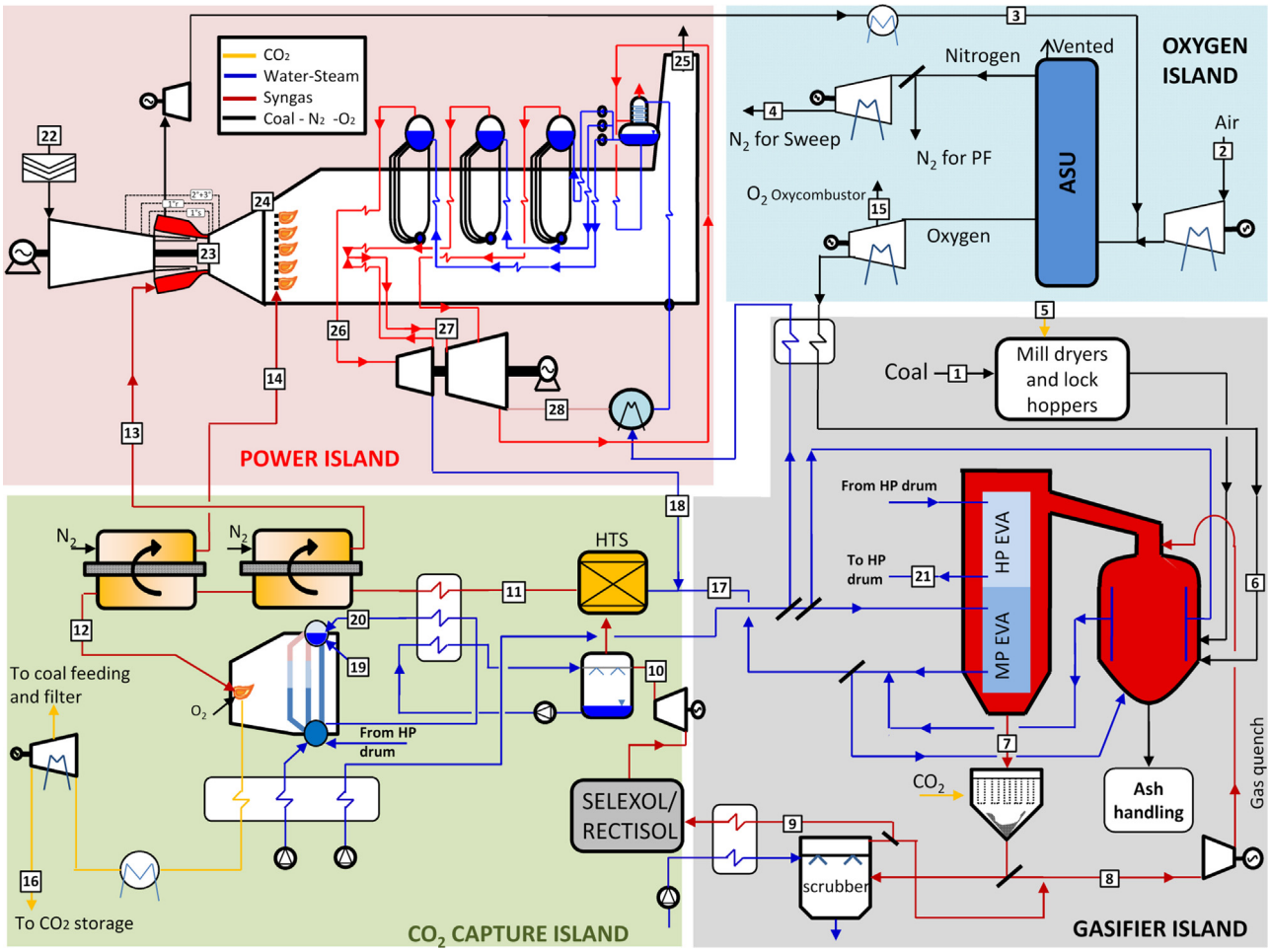

Fig. 5. The layout of an IGCC with capture using a non-sulfur-tolerant membrane and a CO_2 coal charging system. Sulfur removal is based on Rectisol process; hydrogen energy recovery after membrane separation is carried out with oxycombustion. HRSC features the post-firing of flue gas with hydrogen separated at ambient pressure.

maximum membrane temperature, which coincides with the feed inlet temperature (no reaction occurs inside the reactor), is set at 400 °C (Guazzone and Ma, 2008; Peters et al., 2009), requiring a waste heat boiler after the WGS. Higher temperature would reduce the membrane surface area, but it would have no impact on system efficiency since the maximum fuel temperature at combustor inlet is set at 350 °C. Three different values for the Hydrogen Recovery Factors[4] (90%, 95% and 98%) are assumed in order to outline its influence over the electric efficiency and CO_2 capture ratio. The N_2 sweep gas flow rate is set to have an H_2 concentration equal

[4] HRF is defined as the amount of the hydrogen separated divided by the maximum amount of hydrogen that could be separated including CO.

Table 2
Mass, molar and energy balance for the points labelled in Fig. 5 with a HRF of 90%.

Point	T (°C)	P (bar)	G (kg/s)	Q (kmol/s)	Ar	CO	CO_2	H_2	H_2O	H_2S	N_2	O_2
					Molar Fraction (%)							
1	15	44.0	46.8	2.86	Douglas Premium as in Table 4							
2	15	1.01	100.0	3.47	0.9	–	–	–	1.0	–	77.3	20.7
3	30	5.8	100.1	3.47	0.9	–	–	–	0.7		77.5	20.8
4	252	25.0	126.4	4.51	–	–	–	–	–	–	100.0	–
5	80	48.3	51.8	1.18	1.6		96.2	–	–	–	2.0	0.1
6	180	48.0	41.0	1.28	3.1	–	–	–	–	–	1.9	95.0
7	300	41.1	165.5	7.26	1.0	60.6	6.8	21.3	8.8	0.2	1.3	–
8	291	41.1	18.7	0.80	1.0	58.8	9.5	20.7	8.5	0.2	1.3	–
9	164	41.1	121.5	5.30	0.9	53.4	8.6	18.8	17.0	0.2	1.2	–
10	118	54.0	103.3	4.36	1.1	64.9	9.5	22.8	0.1	–	1.5	–
11	507	52.9	200.0	9.72	0.5	5.9	27.4	33.4	32.1	–	0.7	–
12	400	50.3	193.1	6.30	0.8	1.9	49.6	4.5	42.3	–	1.0	–
13	311	25.0	132.4	7.52	–	–	–	40.0	–	–	60.0	–
14	362	1.2	2.1	0.46	–	–	–	90.0	–	–	10.0	–
15	37	49.3	6.9	0.22	3.1	–	–	–	–	–	1.9	95.0
16	28	110.0	85.2	1.95	1.6	–	96.2	–	–	–	2.0	0.1
17	300	54.0	14.1	0.78	–	–	–	–	100.0	–	–	–
18	417	55.9	63.6	3.53	–	–	–	–	100.0	–	–	–
19	335	144.0	52.5	2.92	–	–	–	–	100.0	–	–	–
20	339	144.0	32.4	1.80	–	–	–	–	100.0	–	–	–
21	339	144.0	123.0	6.83	–	–	–	–	100.0	–	–	–
22	15	1.0	632.6	21.93	0.9	–	–	–	1.0	–	77.3	20.7
23	1438	17.6	532.4	19.88	0.6	–	–	–	15.9	–	76.6	6.9
24	593	1.0	665.0	24.47	0.7	–	–	–	13.1	–	76.7	9.5
25	90	1.0	667.1	24.73	0.7	–	–	–	14.6	–	76.1	8.6
26	559	133.9	254.7	14.14	–	–	–	–	100.0	–	–	–
27	559	44.3	191.2	10.61	–	–	–	–	100.0	–	–	–
28	32	0.048	186.9	10.38	–	–	–	–	100.0	–	–	–

to 40% at the reactor outlet. Most of the hydrogen is separated at 25 bar and sent to the GT combustor, while the remaining 10% at ambient pressure is sent for post-firing in the HRSG.

After hydrogen separation, the retentate stream, which consists mainly of CO_2, unconverted H_2 and CO, is burned in oxygen to utilize their heating value. Next, the stream is cooled down to ambient temperature producing HP steam for the HRSG and IP water economization.

As mentioned in Section 1, the inert content in the CO_2 is still significant. At 35 °C, CO_2 molar concentration, by volume on a dry basis, is 96.2% with the balance being inert N_2, Ar and O_2 (which originate in the fuel and the 95% pure oxygen delivered by the ASU). Detailed energy and mass balance for the reference membrane case with HRF = 90% is shown in Table 2.

4.2. Hybrid configuration

As previously mentioned, hybrid feeding does not imply any substantial modification to the plant layout. The main difference compared to the previously discussed case is in the feeding and filter cleaning for the gasification section. Differently from the CO_2 feeding case, there are no technology limits or CO_2 venting dur-ing the charging process. The resulting amount of nitrogen for the lockhoppers is 0.444 kg_{N2}/kg_{coal} while the CO_2 for filters is 0.234 kg_{CO2}/kg_{coal}.

The calculated syngas composition at scrubber outlet was determined while keeping the composition at the outlet of the syngas cooler (see Section 2), then assuming that all the CO_2 for candle filters ends up in the syngas.

The adoption of CO_2 for candle filters increases the CO_2 purity at the membrane outlet from 75.7% to 80.8% (on dry basis). The CO_2 purity is not high enough to perform oxy-combustion and the cryo-genic separation system is therefore adopted. Because of the lower diluent concentration, the CO_2 purity and CO_2 capture increase compared to the pure N_2 feeding: 98.0% and 93.3% vs. 97.4% and 90.1%, respectively.

Another consequence of the cryogenic separation is the recycling of the H_2 and CO, not converted/separated in the membrane modules, to the GT combustor, limiting the thermal power input compared to CO_2 feeding cases.

The hybrid feeding configuration has significant impact on the membrane module working conditions, since the feeding composition is different from both the conventional feeding and the CO_2 feeding cases (Fig. 6 and Table 3).

5. Methodology and assumptions

This section discusses the methodology adopted to evaluate the power cycle performance. Mass and energy balance are estimated using a proprietary computer code Gas and Steam (GS) developed by the GECoS group in the Department of Energy of the Politecnico di Milano to assess the performance of gas/steam cycles, CO_2 capture systems, as well as a variety of other plant options, including IGCC, membranes, advanced CO_2 technologies, etc. (Consonni et al., 1991; Lozza, 1990; Macchi et al., 1995). The plant model is reproduced by assembling components selected from a library containing over 20 basic modules, in a coherent network. Models for these modules had been previously implemented. Built-in rules for efficiency prediction of turbomachines (gas and steam turbine, compressors), as a function of their operating conditions, as well as built-in correlations for predicting gas turbine cooling flows allow the code to generate very accurate estimations of combined cycles performance, even for off-design conditions. The gas turbine model in GS is calibrated to correctly predict the performance of advanced gas turbines, accounting for all the relevant phenomena occurring: fluid-dynamic losses, cooling circuit performance, changes in gas turbine fuel and working fluid composition (Chiesa and Macchi, 2004). The gas turbine simulated is a generic “F Class” and its calibration was already discussed in Manzolini et al. (2012). With respect to natural gas, hydrogen combustion impacts the flame properties, mainly the temperature, flame speed and geometry and results in higher water concentration in the product gases. All these

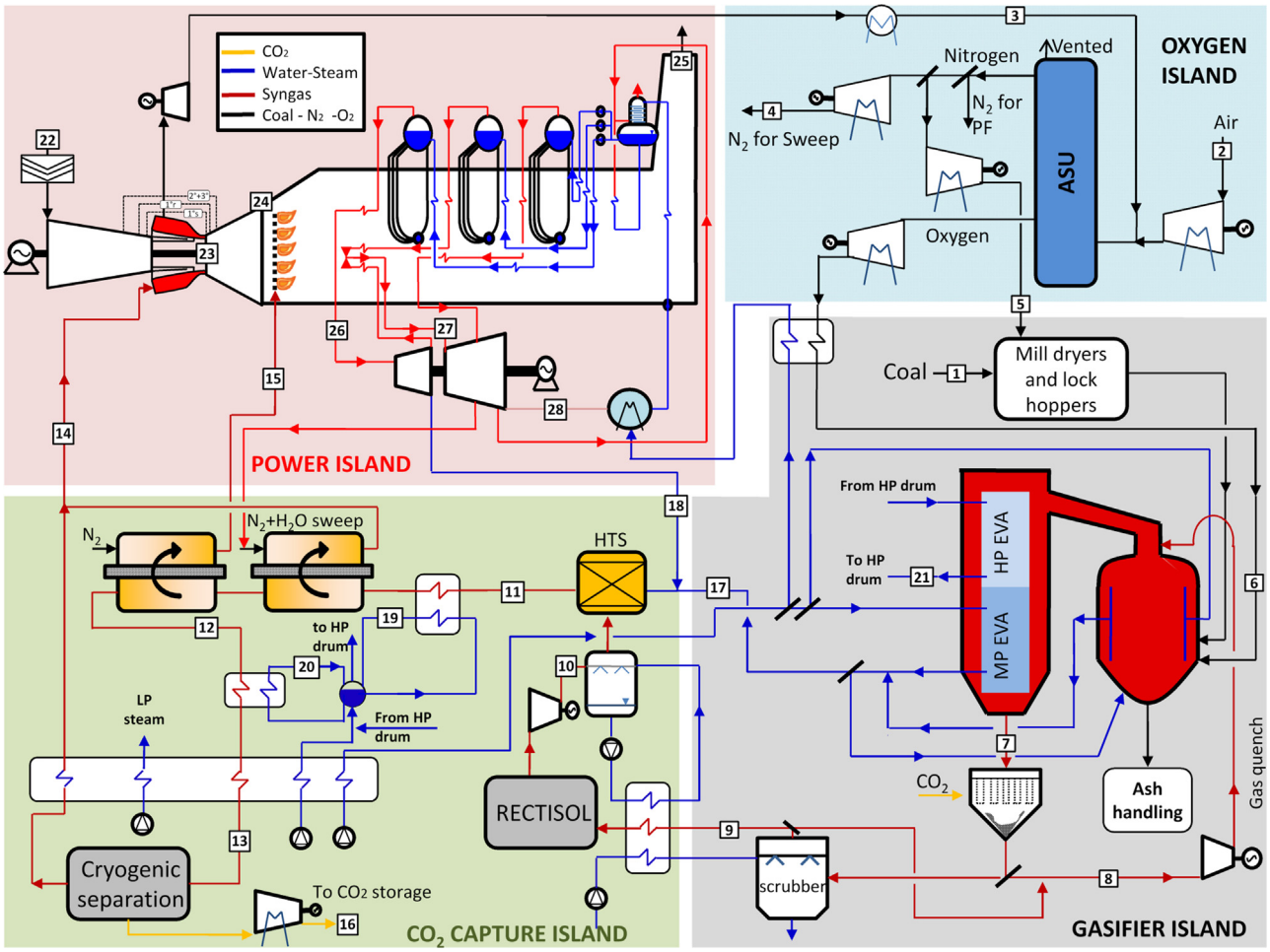

Fig. 6. The layout of an IGCC with capture using a non-sulfur-tolerant membrane and a CO_2–N_2 hybrid coal charging system. Sulfur removal is based on Rectisol process; hydrogen recovery after membrane separation is carried out with cryogenic purification. HRSC features the post-firing of flue gas with hydrogen separated at ambient pressure.

changes, along with the change of the fuel flow rate because of the difference in the LHV, bring about a modification in the machine design specifications. Given that the present work focuses on the potential of membrane application to IGCC with CO_2 capture, it is assumed that the technology level of the gas turbine is kept unchanged (e.g., TIT, pressure ratio) either when hydrogen, syngas or natural gas are adopted. This assumption would require further developments in the gas turbine which could take place if the market of syngas/hydrogen fired GT were to reach a significant size. Furthermore, all the presented cases have the same exhaust gas mass flow featuring the same gas turbine size. The volumetric flow variation at the compressor inlet is reduced thanks to the gas turbine integration with the ASU and is assumed to be controlled with IGV (Inlet Guide Vanes). The resulting variation compared to the design airflow is limited, less than 5%, and the efficiency correction can be neglected.

Another important concern when switching from natural gas to hydrogen is limiting the NO_x emissions. The current industrial practice consists in employing diffusion flame combustors and preventing NO_x formation by diluting the fuel with steam or nitrogen, made available from the steam cycle or an ASU, respectively. As shown in Gazzani et al. (2014a), in order to limit NO_x emissions to less than 20 ppmvd (15% O_2) in a generic heavy duty GT with diffusion flame combustor, it is required to keep the Stoichiometric Flame Temperature (STFT) below 2200 K. Accordingly, in all cases presented in this work the amount of diluting nitrogen has been set to limit the STFT below 2150 K.

The performance of the gasifier and the impact of the feed gas are evaluated using a gasification reduced order model in which gasification kinetics are introduced via a reactor network coupling the mixing and reactions in different parts of the reactor (Monaghan and Ghoniem, 2012).

For the Rectisol and cryogenic CO_2 separation, which are not considered in EBTF, detailed simulations were performed in Aspen Plus® as described in Chiesa et al. (2011) and Gazzani et al. (2014b) (Table 4).

Two important parameters that significantly affect the system performance are the fuel temperature and pressure at the inlet of the gas turbine combustor. A 5 bar overpressure above the air pres-sure is assumed, which results in a sweep gas pressure of 25 bar, while a fuel temperature of 350 °C is taken as reference (EBTF assumptions). Fuel preheating is a current practice to increase the plant efficiency, however, further development would be required to achieve 350 °C. Avoiding fuel cooling and assuming a fuel temperature of 400 °C, the efficiency gain would be of 0.1% point. A similar efficiency variation, but negative in value, can be extended for lower fuel temperatures.

The results of the thermodynamic simulations are expressed in terms of the (net electrical LHV-based) efficiency and CO_2 capture ratio, given respectively by

$$\eta_{el} = \frac{\text{Net power}}{\text{Thermal power input}\ \ (\text{LHV}_{NG})} \quad (1)$$

Table 3
Mass, molar and energy balance for the main points labelled in Fig. 6 with 90% HRF.

Point	T (°C)	P (bar)	G (kg/s)	Q (kmol/s)	Ar	CO	CO_2	H_2	H_2O	H_2S	N_2	O_2
					Molar fraction (%)							
1	15	44.0	41.5	2.54	Douglas Premium as in Table 4							
2	15	1.01	75.5	2.62	0.9	–	–	–	1.0	–	77.3	20.7
3	30	5.8	75.5	2.62	0.9	–	–	–	0.7	–	77.5	20.8
4	253	25.0	92.5	3.30	–	–	–	–	–	–	100.0	–
5	35	48.0	18.3	0.65	–	–	–	–	–	–	100.0	–
6	180	48.0	36.2	1.13	3.1	–	–	–	–	–	1.9	95.0
7	300	41.1	143.9	6.65	0.9	56.4	4.7	26.1	4.5	0.2	7.4	–
8	200	41.1	62.0	2.82	0.8	51.2	6.9	23.7	10.5	0.2	6.7	–
9	156	41.1	101.9	4.66	0.8	49.5	6.7	22.9	13.5	0.2	6.5	–
10	72	54.0	88.9	3.99	0.9	57.7	6.9	26.7	0.1	–	7.6	–
11	489	52.9	167.6	8.36	0.4	5.3	25.5	35.0	30.1	–	3.6	–
12	400	50.3	161.5	5.34	0.7	1.8	46.5	4.7	40.6	–	5.7	–
13	50	48.4	161.5	5.34	0.7	1.8	46.5	4.7	40.6	–	5.7	–
14	323	25.0	128.5	17.07	0.3	1.0	1.7	39.3	10.4	–	47.2	–
15	362	1.2	1.6	0.34	–	–	–	90.0	–	–	10.0	–
16	28	110.0	106.0	2.45	0.4	0.7	96.0	0.6	–	–	2.3	–
17	300	54.0	16.2	0.90	–	–	100.0	–	–	–	–	–
18	418	55.9	56.7	3.15	–	–	100.0	–	–	–	–	–
19	337	144.0	23.1	1.28	–	–	100.0	–	–	–	–	–
20	343	144.0	9.6	0.53	–	–	100.0	–	–	–	–	–
21	345	144.0	105.2	5.84	–	–	100.0	–	–	–	–	–
22	15	1.0	612.1	21.22	0.9	–	–	–	1.0	–	77.3	20.7
23	1440	17.6	528.6	19.87	0.8	–	1.1	–	19.5	–	71.8	6.8
24	687	1.0	666.6	24.79	0.8	–	0.9	–	17.1	–	72.4	8.8
25	90	1.0	666.6	24.79	0.8	–	0.9	–	17.1	–	72.4	8.8
26	559	133.9	193.7	10.75	–	–	100.0	–	–	–	–	–
27	559	44.3	139.1	7.72	–	–	100.0	–	–	–	–	–
28	32	0.048	137.4	7.63	–	–	100.0	–	–	–	–	–

$$\text{CCR} = \frac{\text{CO}_2 \ \text{captured}}{\text{max amount CO}_2 \ \text{produced from fuel used}} \quad (2)$$

Finally, a measure of the energy penalty related to CO_2 capture is given by the Specific Primary Energy Consumption for CO_2 Avoided (SPECCA), already introduced in Campanari et al. (2010), which is defined as

$$\text{SPECCA} = \frac{\text{HR} - \text{HR}_{\text{REF}}}{E_{\text{REF}} - E} = \frac{3600 \cdot ((1/\eta) - (1/\eta_{\text{REF}}))}{E_{\text{REF}} - E} \quad (3)$$

where HR is the heat rate of the plant, expressed in kJ_{LHV}/kWh_{el}; E is the specific CO_2 emission rate, expressed in kg_{CO2}/kWh_{el}; and REF is the reference case for electricity production without carbon capture.

Special attention must be paid to the membrane modelling because of its significant impact on the results. The membrane surface area was determined using a two-dimensional model developed by SINTEF within the CACHET-II project. Mass and energy balance equations for the feed side are discretized using a finite volume method. The radial profiles of the temperature and chemical species concentration are determined. Further details regarding the model adopted can be found in Gazzani et al. (2014b).

6. Thermodynamic results

This section presents the thermodynamic results (see Table 5) for the cases studied in this paper focusing on the impact of the HRF, membrane system layout and gasifier feeding system on the plant performance. In addition, three reference cases are also reported: IGCC based on a Shell gasifier with and without CO_2 capture (as proposed by EBTF, Franco et al., 2011; Gazzani et al., 2013a) and a layout including membranes for hydrogen separation with conventional nitrogen feeding discussed in the previous work (Gazzani et al., 2014b). Focusing on power, it should be noted that higher thermal power input (with respect to the reference case) is needed in the plant with CO_2 capture (about 1100 MW_{th} vs. 900 MW_{th}). This is because of the lower plant efficiency (about 39% for the capture case vs. 47% for the reference plant) and the assumed constant GT size. The same assumption leads to an increase of the thermal power input when low HRF are considered. To a first approximation, a fixed GT size means constant hydrogen mass flow rate to the combustor; therefore an HRF reduction requires more coal at the gasifier inlet. The lower thermal input for the hybrid feeding is because of the cryogenic purification process of the CO_2 stream, where, as anticipated, the unconverted CO and H_2 are sent to the gas turbine instead of the oxy-combustion. Despite its constant size, the GT power output varies significantly with the HRF as is the integration between the ASU and the GT compressor. The lower the HRF, the higher is the amount of oxygen required at the oxy-combustor and consequently the compressed air to the ASU, which reduces the GT net power output.

Regarding the steam cycle, the net power output is significantly higher for the post-firing layout since the energy content of the hydrogen separated at ambient pressure is directly exploited in the post-firing combustor of the HRSG. Similarly, at lower HRF more hydrogen is burned within the oxycombustor: the resulting thermal power is recovered as superheated steam which is expanded in the steam turbine, increasing the power output. When adopting the hybrid feeding system instead of the CO_2-based one, it can be noted that both the steam turbine output and the sweep compressor power decrease. The former is because in the hybrid configuration the retentate is treated in a cryogenic system, hence supplying the hydrogen to the gas turbine combustor. The latter is due to the lower amount of N_2 compressed as sweep: in the hybrid configuration a significant quantity of nitrogen is required to pressurize the lockhopper system thus reducing the available sweep.

Regarding the net electric efficiency, it ranges from 38.7% to 39.8% which means an average efficiency penalty of 8% points for CO_2 capture. In general, high HRF boosts the electric efficiencies because more thermal energy from hydrogen is used in the combined cycle rather than in the steam cycle only. The same concept applies to the electric efficiency penalty in the post-firing cases. However, both cases (i.e., with low HRFs or post-firing)

Table 4
The ambient conditions, fuel characteristics and main component assumptions (Franco et al., 2011, 2010).

Ambient conditions	15 °C/1.013 bar/60% RH			
Air composition, dry molar fraction (%)	N_2 78.08%, CO_2 0.04%, Ar 0.93%, O_2 20.95%			
Douglas premium coal characteristics	C	66.52%	O	5.46%
Ultimate analysis	N	1.56%	Chlorine	0.009%
	H	3.78%	Moisture	8.0%
	S	0.52%	Ash	14.15%
Coal LHV, HHV	25.17 MJ/kg, 26.23 MJ/kg			
CO_2 specific emission	349.0 (g/kW h_{LHV})			
Gas turbine				
Pressure ratio	18.1			
Gas mass flow rate at the turbine outlet	665 kg/s			
Stoichiometric flame temperature	<2150 K			
TIT	1360 °C			
Pressure loss at inlet	1 kPa			
Heat recovery steam cycle (HRSC)				
Pressure levels, bar	144, 54, 4			
Maximum temperature SH e RH	565 °C			
Pinch, subcooling, approach ΔT	10/5/25 °C			
Condensing pressure	0.048 bar (32 °C)			
Turbine isentropic efficiency (HP/IP/LP)	92/94/88%			
Pumps efficiency	70%			
HRSG thermal losses	0.7% of thermal input			
HRSG pressure losses, gas side	4 kPa			
Gas turbine and steam cycle				
Generator efficiency	98.7%			
Mechanical efficiency	99.6%			
Power consumed for heat rejection	0.8% of heat released			
Air separation unit				
Oxygen purity	95%			
Nitrogen purity	99%			
Oxygen outlet temperature	20 °C			
Oxygen temperature entering the gasifier	180 °C			
Oxygen pressure entering the gasifier	48 bar			
Oxygen and nitrogen temperature leaving ASU	22 °C			
Gasification section				
Gasifier outlet pressure	44 bar			
Gasifier outlet temperature	1550 °C			
Coal conversion	99.3%			
Heat to membrane walls (% of thermal $input_{LHV}$)	0.9%			
O/C ratio	0.44			
Dry quench exit temperature	900 °C			
Scrubber inlet temperature	298 °C			
Selexol process (H_2S removal)				
Electrical energy consumption	0.538 kW h/kg_{H2S}			
Thermal energy consumption	5.82 kW h/kg_{H2S}			
CO_2 venting	1.42 mol CO_2/mol H_2S			
Rectisol process (H_2S removal)				
Electrical energy consumption	7.49 kW h/kg_{H2S}			
Thermal energy consumption	16.72 kW h/kg H_2S			
CO_2 venting	6.62 mol CO_2/mol (H_2S + COS)			
CO_2 separation and compression				
Final delivery pressure	110 bar			
Compressor isentropic efficiency	85%			
Temperature for CO_2 liquefaction	25 °C			
Pressure drop for intercoolers and dryer	1.0%			
Pump efficiency	75%			
CO_2 purity	>96%			

take advantage of the lower membrane surface area thanks to the higher permeation driving force at the feed outlet, which is the most critical section (see Table 5). Indeed, low HRF allows keeping a higher H_2 concentration at the feed-side outlet while post-firing increases the absolute pressure difference. In particular, in the latter case, the required membrane surface area drops of about 50% thanks to the low permeate pressure of the last module. Eventually, it can be noted that the efficiency results of the CO_2/hybrid and the N_2 feeding cases differ of about 0.1–0.5 percentage points: this is mainly because of the different arrangement of the heat recovery section as consequence of the retentate purification processes.

Comparing the two feeding concepts, there are significant advantages for the hybrid configuration because: (i) the hydrogen partial pressure at the membrane inlet is higher (35.0% vs. 33.4%), and (ii) the higher CO_2 content in the CO_2 feeding case limits the WGS equilibrium, and hence it reduces the H_2 concentration. This advantage is outlined in Fig. 7 where the membrane area required for kmol of H_2 permeated is shown. From the same picture, the increase of membrane surface area with the HRF can be noted. On the other hand, the hybrid feeding case requires the addition of steam as a sweep gas because the N_2 available is not enough to guarantee an H_2 concentration of 40% at the membrane outlet. In

Table 5
Power balances for the investigated cases and two reference cases.

		Shell no-cap	Shell Selexol	Membrane plants with Rectisol H_2S removal								
Coal gas carrier and feeding				N_2	CO_2						Hybrid CO_2–N_2	
Membrane module config.				Post-firing	No post-firing			Post-firing			Post-firing	
HRF				0.90	0.90	0.95	0.98	0.90	0.95	0.98	0.90	0.95
Thermal power input	(MW)	896.6	1044.4	1104.4	1097.6	1049.7	1022.7	1253.5	1177.0	1133.2	1106.0	1115.1
Power production												
Gas turbine	(MW)	290.2	305	315.8	308.3	314.9	319.0	302.8	308.1	312.9	315.6	320.0
Steam cycle gross power	(MW)	197.7	179.2	223.2	232.7	202.4	182.7	303.3	266.7	238.3	219.5	219.4
Expander ASU	(MW)	8.5	10.2	10.6	12.2	10.9	10.2	14.0	12.3	11.3	10.6	10.7
Auxiliaries consumptions												
Coal handling	(MW)	1.7	1.9	2.1	2.0	2.0	1.9	2.3	2.2	2.1	2.1	2.1
Ash handling	(MW)	0.5	0.6	0.6	0.6	0.6	0.6	0.7	0.7	0.6	0.6	0.6
Sulphur adsorption	(MW)	0.4	19.3	4.9	6.4	6.1	5.9	7.4	7.0	6.7	4.7	4.8
Cryogenic system	(MW)	–	–	10.2	–	–	–	–	–	–	10.7	10.7
Lock hopper compressor	(MW)	9.2	11.1	13.0	–	–	–	–	–	–	10.3	10.4
Sweep compressor	(MW)	32.1	24	41.7	59.8	54.4	50.6	59.8	59.8	55.0	43.8	44.1
ASU + O_2 compression	(MW)	22.7	26.6	28.2	33.1	29.6	27.5	38.1	33.3	30.6	28.2	28.4
Gasifier blower	(MW)	1.1	1.3	1.3	1.1	1.0	1.0	1.3	1.2	1.1	1.3	1.3
CO_2 compressor	(MW)	0.0	22.9	–	3.1	3.0	2.9	3.5	3.3	3.2	–	–
Feed compressor	(MW)	0.0	–	4.5	4.4	4.2	4.1	5.1	4.7	4.5	4.5	4.5
Heat rejections	(MW)	2.5	2.5	2.8	3.6	3.2	2.9	4.1	3.9	3.6	3.1	3.0
BOP	(MW)	0.7	1.3	1.1	2.3	2.0	1.9	2.6	2.3	2.1	1.2	1.3
Net power output	(MW)	422.4	375.9	435.4	434.0	419.5	410.1	491.3	465.0	449.5	431.5	435.2
Efficiency	%	47.1	36.00	39.1	39.2	39.6	39.7	38.9	39.2	39.3	38.7	38.7
Advanced												
Specific emissions	(g/kWh)	–	–	–	12.5	12.3	12.3	12.8	12.7	12.7	–	–
Carbon capture avoided	(%)	–	–	–	98.3	98.3	98.3	98.3	98.3	98.3	–	–
SPECCA	(MJ/kgCO_2)	–	–	–	2.1	2.0	2.0	2.3	2.2	2.1	–	–
Actual												
Specific emissions	(g/kWh)	732.1	98.5	104.4	277.8	275.2	274.7	280.4	278.7	277.9	90.5	77.9
Carbon capture avoided	(%)	–	86.5	85.7	62.1	62.4	62.5	61.7	61.9	62.0	87.6	89.4
SPECCA	(MJ/kgCO_2)	–	3.71	2.5	3.4	3.2	3.1	3.6	3.4	3.3	2.6	2.5
Efficiency penalty	%	–	11.10	8.02	7.92	7.49	7.37	8.26	7.95	7.79	8.44	8.43
Membrane area	(m^2)	–	–	14 297	29 334	85 907	197 804	22 769	54 019	126 145	19 407	45 079

Table 6
Equipment cost references for the main components.

Plant component	Scaling parameter	Reference erected cost C_0 (M€)	Reference size, S_0	Scale factor	N
Gasification section					
Coal handling[a,b]	Coal input (kg/s)	27.5	32.9	0.67	1
Ash handling [a,b]	Ash flow rate (kg/s)	4.7	9.7	0.6	1
Gasifier[a,b],	Thermal input (MW)	90.0	828.0	0.67	1
Air separation unit (ASU)[a,b]	Oxygen produced (kg/s)	26.6	28.9	0.7	1
Power section					
Gas turbine, generator and auxiliaries[a,b,c]	$GT_{Net\ Power}$ (MW)	49.4	272.12	0.3	1
HRSG, ducting and stack[a,b,c]	U*S (MW/K)	32.6	12.9	0.67	1
Steam turbine, generator and auxiliaries[a,b,c]	$ST_{Gross\ Power}$ (MW)	33.7	200.0	0.67	1
Cooling water system and BOP [a,b,c] Nitrogen	Q_rejected (MW)	49.6	470.0	0.67	1
compressor for GT dilution [b]	Compressor power (MW)	14.8	47.6	0.67	1
Gas conditioning and CO_2 separation section					
Low temperature heat recovery (LTHR)[a,b]	Thermal input (MW)	6.1	828.0	0.67	1
Selexol Acid Gas Removal (AGR)[a,b] Rectisol	Coal input (kg/s)	12.0	32.9	0.67	1
Acid Gas Removal (AGR)[a,b]	Coal input (kg/s)	13.5	32.9	0.67	1
Water treatment[b]	Coal input (kg/s)	10.7	32.9	0.67	1
Claus[b]	Sulphur flow rate (kg/s)	8.0	0.2	0.67	1
Water gas shift reactors[b]	Thermal input (MW)	11.7	954.1	0.67	2
Selexol CO_2 separation system[a,b]	CO_2 captured (kg/s)	28.1	69.4	0.8	1
CO_2 compressor and condenser[a,b]	Compressor power (MW)	9.9	13.0	0.67	1
Oxy combustor[a,b]	Oxygen Input (kg/s)	1.29	3	1	1

[a] DOE/NETL-2011/1498 (2011).
[b] Franco et al., 2011 (2010).
[c] Gas Turbine World Handbook (2010).

the CO_2 feeding case, this does not occur since the amount of N_2 available is higher (no N_2 is used for the lockhopper).

As discussed in Section 2, two different scenarios could be considered for the CO_2 feeding system: in the actual system, part of the CO_2 used for fuel charging is vented (which is the current N_2 feeding technology), whereas in an advanced scenario, all the CO_2 is recovered. In the former case, the CO_2 vented strongly penalizes the CO_2 avoidance with values of CO_2 avoided of about 70%, making this configuration less attractive. To the contrary, if all the CO_2 could be recovered, avoidance higher than 98% might be achieved (in the reference case the CO_2 avoidance is about 86%). The hybrid configuration doesn't have this issue and the calculated CO_2 avoidance is between 87% and 90%.

The resulting SPECCA for the CO_2 feeding is in the range of 2.0–2.1 MJ/kg$_{CO2}$ when the advanced scenario is considered and between 3.1 and 3.6 MJ/kg$_{CO2}$ with the actual configuration. The SPECCA for the hybrid configuration stands in the middle of these two limits and, similarly to the membrane case with conventional N_2 feeding, is 2.5 MJ/kg$_{CO2}$. In comparison, the SPECCA for the reference IGCC with CO_2 capture using Selexol is 3.6 MJ/kg$_{CO2}$, therefore Pd-based membrane integration could lead to significant improvements in IGCC CO_2 capture technologies.

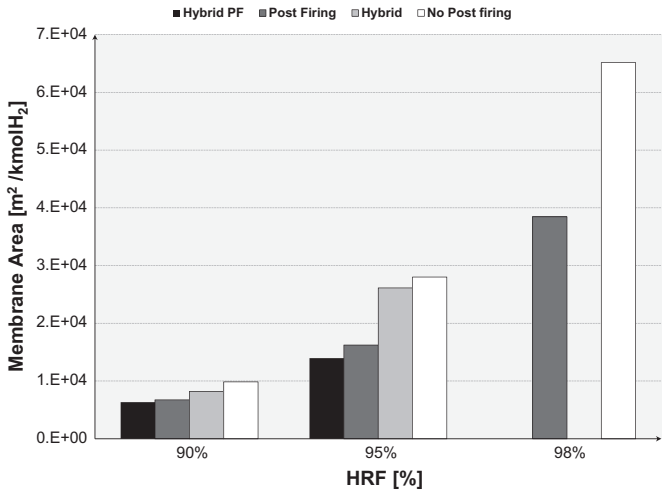

Fig. 7. The membrane surface area required per kmol of H_2 permeated. Cases are divided as function of the HRF and plant configuration; moving from the left bar towards right: hybrid feeding with post firing (90 and 95 HRF), CO_2 feeding with post firing (90, 95 and 98 HRF) hybrid feeding without post firing (90 and 95 HRF) and CO_2 feeding without post firing (90, 95 and 98 HRF).

Table 7
O&M and consumable costs (PH3/14, 2000; PH4/33, 2004) (Manzolini et al., 2013).

Coal costs	€/GJ_{LHV}	3
O&M		
Labour costs for IGCC cases	M€	8.9
Maintenance	% of total plant cost	1
Insurance	% of total plant cost	1
Consumables		
Evaporative tower blow-off	% of evaporated water	100
Cooling water make-up costs	€/m^3	0.35
HRSG water blow-off	% of steam produced	1
Process water costs	€/m^3	2
Rectisol	%Equipment cost	2
Catalyst replacement		
Water gas shift lifetime	Years	5
Water gas shift cost	k€/m^3	14

7. Economic assessment

The economic assessment is based on the European Benchmarking Task Force methodology (Franco et al., 2011, 2010). Different from other approaches (Rubin, 2012), this methodology considers only capture costs, hence neglecting transport and storage costs; the aim of the methodology is not to determine the exact cost of CO_2 avoided, but to compare in a consistent way different capture technologies. The cost of electricity (COE)[5] is calculated by setting the net present value (NPV) of the power plant to zero as adopted in IEAGHG models (PH3/14, 2000; PH4/33, 2004). This can

[5] The cost of electricity is different from the price of electricity since it does not include any revenues and consequently taxes.

Table 8
Component costs, total equipment cost, total plant cost and specific investment costs for the main cases considered in this work. Costs are in M€.

	Shell no cap	Shell Selexol	Membrane plants with Rectisol H_2S removal							
Coal gas carrier and feeding			N_2	CO_2				Hybrid		
Membrane module config			Post firing	No post-firing	Post firing			No post-firing	Post firing	
HRF (%)	90	90	90	90	90	95	98	90	90	95
Coal handling	28.8	32.1	31.9	31.8	34.8	33.4	32.5	30.2	32.0	32.2
Gasifier	94.4	105.1	109.1	108.7	118.8	113.9	111.1	103.0	109.3	109.9
Gas turbine	50.4	51.1	51.6	51.3	51.0	51.3	51.5	51.9	51.6	51.9
Steam turbine	33.4	31.3	36.2	37.6	44.9	41.2	38.2	31.2	36.3	36.3
HRSG	36.4	40.0	39.1	37.6	40.1	40.7	38.3	40.9	42.1	43.5
LTHR	6.4	7.1	7.3	7.3	8.0	7.7	7.5	6.9	7.4	7.4
Heat rejection	37.5	41.9	40.6	48.3	52.8	51.3	48.2	35.4	43.3	42.8
ASU	29.6	33.1	35.8	35.7	39.2	37.5	36.5	33.8	35.9	36.1
ASH	10.1	11.1	11.5	11.5	12.4	12.0	11.7	10.9	11.5	11.6
AGR	14.1	14.0	15.6	15.6	17.1	16.4	16.0	14.8	15.7	15.8
Gas cleaning	4.0	4.5	4.6	4.6	5.1	4.9	4.7	4.4	4.7	4.7
Water treatment	11.2	12.5	12.4	12.3	13.5	12.9	12.6	11.7	12.4	12.5
Claus	8.4	9.3	10.0	10.0	11.0	10.5	10.2	9.5	10.1	10.1
WGSR	–	12.5	–	–	–	–	–	–	–	–
Selexol	–	33.6	–	–	–	–	–	–	–	–
CO_2 compressor	–	14.5	8.4	3.8	4.1	4.0	3.9	8.3	8.7	8.7
Membrane	–	–	82.9	170.1	132.1	313.3	731.6	140.1	112.6	261.5
Nitrogen compressor dilution	11.3	9.3	16.2	17.2	17.2	17.2	16.3	15.2	16.1	16.2
Saturator	0.2	0.2	0.2	0.2	0.3	0.3	0.2	0.2	0.2	0.2
HTS	–	–	4.4	4.4	4.9	4.7	4.5	4.2	4.5	4.5
ASU expansor	–	–	6.7	5.2	5.7	5.2	4.9	4.4	4.7	4.7
Cryogenic purification	–	–	0.9	–	–	–	–	0.8	0.9	0.9
Oxycombustor	–	–	–	2.5	3.0	1.5	0.6	–	–	–
LT heat exchanger	–	–	3.4	7.6	7.6	7.4	7.2	2.0	2.0	1.4
HT heat exchangers	–	–	8.4	7.4	7.4	7.5	6.1	1.8	1.8	1.8
Total equipment cost	376.2	463.4	538.3	631.1	631.0	794.6	1194.5	561.9	563.8	714.6
Total plant cost	**887.9**	**1093.6**	**1270.2**	**1489.2**	**1489.0**	**1875.0**	**2818.8**	**1326.0**	**1330.6**	**1686.4**
Net power output (MW)	422.4	379.6	435.4	434.0	491.3	465.0	449.5	401.7	431.5	435.2
Net electric efficiency(%)	47.1	36.0	39.0	39.2	38.9	39.2	39.3	39.3	38.7	38.7
CO_2 avoided (%)	–	86.5	85.7	98.3	98.3	98.3	98.3	89.4	87.6	89.4
Specific costs (€/kW_{gross})	1788.8	2212.4	2311.3	2691.8	2401.1	3194.1	5011.2	2621.4	2438.4	3065.5
Specific costs (€/kW_{net})	**2101.8**	**2881.0**	**2917.1**	**3431.3**	**3030.7**	**4032.1**	**6270.6**	**3301.2**	**3083.5**	**3875.3**

be achieved by varying the plant COE until the revenues balance the cost over the entire lifetime of the power plant.

The total plant cost is calculated using the bottom-up approach (BUA) that is frequently used when innovative plants without construction experiences are evaluated. The approach starts by calculating the Total Direct Plant Cost (TDPC) from the equipment costs, then adding installation costs as piping, erection, Outside Battery Limits (OBL), etc. Total direct plant costs plus indirect costs (IC), which are calculated as a percentage of direct plant costs, lead to Engineering, Procurement and Construction costs (EPC). Finally, Total Plant Cost (TPC) results from EPC plus owner's cost and contingencies.

The equipment cost database is summarized in Table 6. Most of the other data used for the gasification island are taken from Franco et al. (2011, 2010) and are consistent with DOE/NETL-2011/1498 (2011). Regarding the power section, the GT specific costs are calculated as an average of F-Class gas turbine (Gas Turbine World Handbook, 2010). A constant mass flow rate at the turbine outlet is assumed for all cases, which therefore have the same size except for the generator power output; this results in a low scale factor of 0.3. Combustor modifications required by syngas combustion are not taken into account due to the difficulty in predicting correct figures.

Rectisol and Selexol costs were determined according to a bottom-up approach, starting from the data presented in Doctor et al. (1993) and carrying out a preliminary sizing of each process component. For a defined quality of coal feedstock, the AGR cost is scaled using the amount of coal treated (or the thermal power input).

Membrane module costs are assumed to be proportional to the surface area and equal to 5800 €/m^2. They are based on a design with 19 membrane tubes for a total surface area for each module of about 10 m^2 as proposed by Technip within CACHET-II project (Song and Forsyth, 2013). Costs include membrane tubes, sealing, vessel materials and manufacturing. Lifetime of membrane tubes is equal to five years, while the membrane vessel itself is assumed to be recycled.

Labour costs are typical of an average European social environment. About O&M costs, the IEAGHG methodology[6] was adopted (PH3/14, 2000; PH4/33, 2004) assuming that the coefficients are calibrated towards EBTF figures (Table 7).

8. Economic results

Equipment and total plant costs for the most interesting cases investigated are shown in Table 8 together with the reference cases. Only two cases without post-firing are reported to outline the advantages of the post-firing configuration or the large membrane areas penalties. Among all cases shown, equipment costs are quite similar except for: (i) the gasifier, (ii) the steam turbine and (iii) the membrane modules. The gasifier cost is proportional to the thermal input, therefore it decreases for high HRF and for the hybrid feeding. Regarding the steam turbine, the cost depends on the power output which, for the CO_2 feeding case, increases at low HRF: the lower the

[6] The IEA methodology assumes that fixed costs as maintenance and insurance are function of the total plant costs.

Table 9
Comparison between the membrane cases and the reference cases in terms of cost of electricity and the cost of CO_2 avoided. Total COE is subdivided into four main parts: investment, fixed O&M, consumables and fuels.

	Shell no cap	Shell Selexol	Membrane plant with Rectisol H_2S removal							
			CO_2 feeding						Hybrid feeding	
			No post-firing			Post firing			Post firing	
HRF (%)	90	90	90	95	98	90	95	98	90	95
Investment cost (€/MWh)	34.5	47.5	56.4	86.9	149.4	49.9	66.3	103.0	50.7	63.7
Fixed O&M costs (€/MWh)	7.1	9.0	9.7	13.6	21.4	8.6	10.8	15.4	9.0	10.6
Consumables (€/MWh)	1.8	2.2	6.8	14.0	28.8	5.6	9.3	18.1	5.4	8.5
Fuel costs (€/MWh)	22.9	30.0	27.6	27.3	27.2	27.8	27.6	27.5	27.9	27.9
COE (€/MWh)	66.3	88.6	100.5	141.8	226.8	91.8	113.9	163.9	93.1	110.8
Cost of CO_2 avoided (€/tCO_2), state-of-the-art lock hopper	**–**	**36.7**	**75.2**	**165.2**	**350.8**	**56.4**	**105.0**	**214.9**	**41.8**	**68.0**
Cost of CO_2 avoided (€/tCO_2), advanced lock hopper	**–**	**–**	**47.5**	**104.9**	**222.9**	**35.4**	**66.2**	**135.7**	**41.8**	**68.0**

HRF, the higher the retentate thermal power which is then utilized in the steam turbine. The membrane cost is proportional to the surface area; therefore, the membrane costs for HRF 98% are six times the HRF 90% case, and the post-firing layout has 25% membrane cost reduction as compared to the entirely H_2 separation at high pressure.

For the 90% HRF case, which shows the lowest membrane surface area, membrane share cost is 20%, which is even higher than the gasifier.

The membrane cost has a significant impact on the overall plant in the post-firing configuration as well, leading to specific costs from 3000 €/kW to more than 6000 €/kW. Cases without post-firing are even more expensive: at the same HRF (90%), the specific costs increase by 10%. On the other hand, the specific costs for the reference IGCC without capture is equal to 2100 €/kW, while with capture is 2900 €/kW, therefore, from this perspective, the membrane cases are penalized. Compared to the membrane application in IGCC with N_2 feeding, the two feeding technologies investigated in this work are more expensive, mainly because of the larger membrane surface area required.

The cost of electricity and the cost of CO_2 avoided are summarized in Table 9. It should be recalled that two different feeding scenarios are considered for the CO_2 case: the actual, with part of CO_2 necessary for coal charging vented, and the advanced where all the CO_2 is recovered. Results show that only the advanced scenario with 90% HRF leads to interesting results with cost of CO_2 avoided of about 35.4 €/t_{CO2} vs.56.4 €/t_{CO2}. Compared to the reference case, membranes are penalized for investment (i.e., membrane module costs and consumables as membrane substitution), while there is significant advantage in terms of fuel costs. The situation worsens at higher HRF and for the layout without post-firing. The hybrid layout shows a cost of CO_2 avoided in between the actual and advanced scenario since it has no significant differences in terms of cost and efficiency and the CO_2 avoidance is in between. For the hybrid concept, the cost of CO_2 avoided does not depend on technology development, but it is based on actual performances.

As a general comment, only the membrane layout with post-firing, which is a novel concept introduced for the first time in this paper, has good potential as a CO_2 capture technology in IGCC. Moreover, these results are achieved with a very conservative cost of the membrane reactor (5800 €/m^2). Therefore, a sensitivity analysis on membrane costs was performed in order to assess its impact on the CO_2 avoided cost. This analysis is performed on the most promising configuration: the post firing cases and feed pressure of 54 bar, both for CO_2 and Hybrid feeding. The results of this analysis are depicted in Fig. 8. It can be seen that halving the membrane

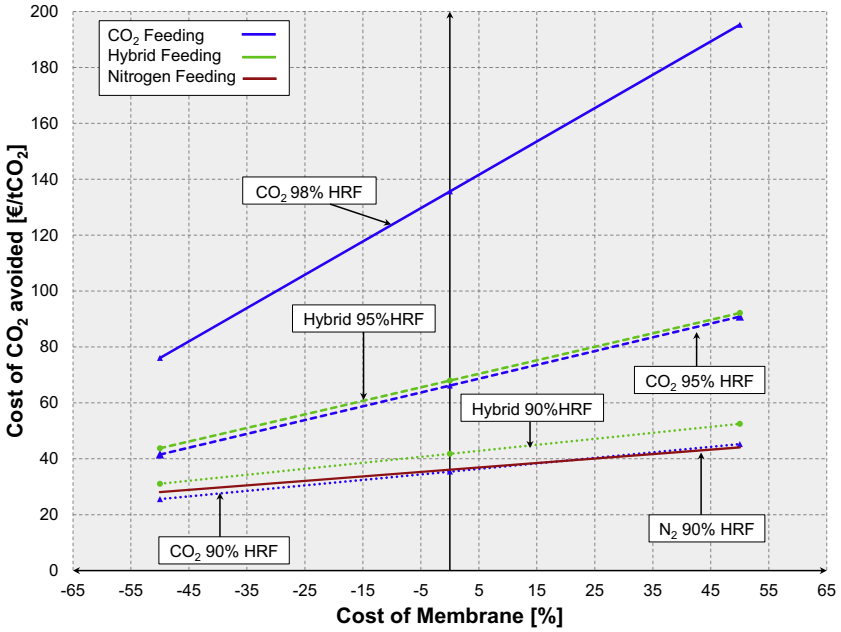

Fig. 8. Cost of CO_2 avoided for membrane cases at different membrane module cost compared to reference value.

Table 10
Performance and cost for different steam temperatures.

Membrane integration with CO_2 feeding and post firing		
HRF (%)	90	90
T steam HRSG	565	620
Total equipment cost	631.0	643.7
Total plant cost	**1489.0**	**1519.1**
Net power output (MW)	491.3	501.1
Net electric efficiency (%)	38.9%	39.3%
CO_2 avoided (%)	98.3%	98.3%
Specific costs (€/kW_{gross})	2401.1	2408.4
Specific costs (€/kW_{net})	**3030.7**	**3031.2**
Investment cost (€/MWh)	49.9	49.9
Fixed O&M costs (€/MWh)	8.6	8.5
Consumables (€/MWh)	5.6	5.5
Fuel costs (€/MWh)	27.8	27.5
COE (€/MWh)	91.8	91.3
Cost of CO_2 avoided (€/tCO_2), state-of-the-art lock hopper	**56.4**	**55.0**
Cost of CO_2 avoided (€/tCO_2) advanced lock hopper	**35.4**	**34.8**

cost, the cost of CO_2 avoided can be reduced by 25% reaching values of about 30 €/t_{CO2}, slightly cheaper than the reference commercial technologies (37 €/t_{CO2}). However, given the process novelty and the cost uncertainties of the advanced components (e.g., oxy-combustor and cryogenic purification), the economic assessment should not be considered as an ultimate result but as an indication for future research topics.

An additional assessment was performed to investigate the influence of the maximum temperature of the steam cycle from 565 to 620 °C. This calculation was carried out for the CO_2 feeding case with post-firing at 90% HRF. The post-firing configuration allows the adoption of higher steam temperatures in the HRSG, compared to the conventional GT based cycle, thanks to the higher temperature of the exhaust gases (this is not possible with conventional gas turbines where the turbine outlet temperature is below 600 °C). Higher steam temperatures have negligible impact on the plant cost even with the stipulated 20% increase of the HRSG cost for 620 °C, while it pushes the net electric efficiency as shown in Table 10. The resulting cost of electricity and CO_2 avoided reduces by 2%.

9. Conclusions

This work focuses on the application of hydrogen selective membranes in Integrated Gasification Combined Cycle with "CO_2 coal feeding". In contrast to the previous work, a reduced order modelling approach has been adopted for the simulation of the CO_2 feeding gasifier. The membrane model was developed inside the CACHET-II project for the prediction of the membrane area necessary in each power plant configuration.

Built upon previous work (Gazzani et al., 2014b), the study was focused on an innovative layout, where part of the hydrogen is separated at low pressure to post-fire the HRSG. High pressure H_2 is fed to the gas turbine. This configuration significantly reduces the membrane surface area, while keeping a satisfactory efficiency. The membrane configuration achieves high efficiency and high CO_2 avoided, reducing the efficiency penalty and, because it uses oxy-combustion of the membrane retentate, it eliminates the need for a cryogenic system. The adoption of CO_2 feeding requires advancement in lockhopper management in order to limit CO_2 venting which strongly penalizes the CO_2 avoidance as well as economics.

A sensitivity analysis shows that the cost reduction of the membrane module is the key factor for future economic improvement. Finally, compared to other innovative technologies for CO_2 capture, membranes exhibit high potential for reducing the economic penalties making their development at a commercial scale an important contribution to the deployment of the technology. It is worth noting that further advancements are required in terms of reliability and stability of the membrane as well as their tolerance to H_2S.

Acknowledgement

The CACHET-II project has received funding from the European Community's Seventh Framework Programme FP7/2007-2013 under Grant agreement no. 241342.

References

Abani, N., Ghoniem, A., 2013. Large-eddy simulation of coal gasification in an entrained flow gasifier. Fuel 104, 664–680.
Amrollahi, Z., Ertesvåg, I.S., Bolland, O., 2011. Optimized process configurations of post-combustion CO_2 capture for natural-gas-fired power plant – exergy analysis. Int. J. Greenh. Gas Control 5, 1393–1405.
Anantharaman, R., Bolland, O., 2011. Integration of oxygen transport membranes in an IGCC power plant with CO_2 capture. Chem. Eng. Trans. 25, 25–30.
Botero, C., Brasington, R., Field, R., Herzog, H., Ghoniem, A., 2012. Performance of an IGCC plant with carbon capture and coal-CO_2-slurry feed: impact of coal rank, slurry loading and syngas cooling technology. Ind. Eng. Chem. Res. 51, 1178–11790.
Botero, C., Field, R., Herzog, H., Ghoniem, A., 2013. Impact of finite-rate kinetics on carbon conversion in a high-pressure single-stage entrained flow gasifier with coal-CO_2 slurry feed. J. Appl. Energy 104, 408–417.
Bredesen, R., Jordal, K., Bolland, O., 2004. High-temperature membranes in power generation with CO_2 capture. Chem. Eng. Process. Process Intensif. 43, 1129–1158.
Campanari, S., Chiesa, P., Manzolini, G., 2010. CO_2 capture from combined cycles integrated with molten carbonate fuel cells. Int. J. Greenh. Gas Control 4, 441–451.
Casas, N., Schell, J., Joss, L., Blom, R., Mazzotti, M., 2012. A novel adsorbent material (MOF/MCM-41) for pre-combustion CO_2 capture by pressure swing adsorption. In: GHGT-11 Conference Proceedings, Kyoto, 19–23 November 2012.
Chen, L., Yong, S., Ghoniem, A., 2012. Oxy-fuel combustion of coal for carbon capture: characterization, fundamentals, stabilization and CFD modeling. Prog. Energy Combust. Sci. 38, 156–214.
Chiesa, P., Campanari, S., Manzolini, G., 2011. CO_2 cryogenic separation from combined cycles integrated with molten carbonate fuel cells. Int. J. Hydrogen Energy 36, 10355–10365.
Chiesa, P., Kreutz, T.G., Lozza, G.G., 2007. CO_2 sequestration from IGCC power plants by means of metallic membranes. J. Eng. Gas Turbines Power 129, 123.
Chiesa, P., Macchi, E., 2004. A thermodynamic analysis of different options to break 60% electric efficiency in combined cycle power plants. J. Eng. Gas Turbines Power 126, 770.
Consonni, S., Lozza, G., Macchi, E., Chiesa, P., Bombarda, P., 1991. Gas Turbine-Based Cycles for Power Generation. Part A: Calculation Model.
Van Dijk, E., Walspurger, S., Cobden, P., Van Den Brink, R., 2011. Testing of hydrotalcite based sorbents for CO_2 and H_2S capture for use in sorption enhanced water gas shift. Int. J. Greenh. Gas Control 5, 505–511.
Doctor, R.D., Molburg, J.C., Thimmapuram, P., Berry, G.F., Livengood, C.D., Johnson, R.A., 1993. Gasification combined cycle: carbon dioxide recovery, transport, and disposal. Energy Convers. Manage. 34 (9–11), 1113–1120.
DOE, 2007. Carbon Sequestration Technology Roadmap and Program Plan.
DOE/NETL-2011/1498, 2011. Cost and Performance of PC and IGCC Plants for a Range of Carbon Dioxide Capture.
Franco, F., Anantharaman, R., Bolland, O., Booth, N., Van Dorst, E., Ekstrom, C., 2010. Common framework and test cases for transparent and comparable techno-economic evaluations of CO_2 capture technologies – the work of the European Benchmarking Task Force 00., pp. 1–8.
Franco, F., Anantharaman, R., Bolland, O., Booth, N., Dorst, E., Van Ekstrom, C., 2011. European Best Practice Guide for Assessment of CO_2 Capture Technologies.
2010. Gas Turbine World Handbook.
Gazzani, M., Chiesa, P., Martelli, E., Sigali, S., Brunetti, I., 2014a. Using hydrogen as gas turbine fuel: premixed versus diffusive flame combustors. J. Eng. Gas Turbines Power 136, 051504.
Gazzani, M., Macchi, E., Manzolini, G., 2013a. CO_2 capture in integrated gasification combined cycle with SEWGS – Part A: thermodynamic performances. Fuel 105, 206–219.
Gazzani, M., Manzolini, G., Macchi, E., Ghoniem, A.F., 2013b. Reduced order modeling of the Shell–Prenflo entrained flow gasifier. Fuel 104, 822–837.
Gazzani, M., Turi, D.M., Manzolini, G., 2014b. Techno-economic assessment of hydrogen selective membranes for CO_2 capture in integrated gasification combined cycle. Int. J. Greenh. Gas Control 20, 293–309.
Guazzone, F., Ma, Y.H., 2008. Leak growth mechanism in composite Pd membranes prepared by the electroless deposition method. AIChE J. 54, 487–494.

Guo, X., Lu, W., Zhengua, D., Liu, H., Gong, X., Li, L., Honglin, Z., Guo, B., 2012. Experimental investigation into a pilot-scale entrained-flow gasification of pulverized coal using CO_2 as carrier gas. Energy Fuels 26, 1063–1069.

Hong, J., Field, R., Gazzino, M., Ghoniem, A., 2010. Operating pressure dependence of the pressurized oxy-fuel combustion power cycle. Energy 35, 5391–5399. Hong, J., Kirchen, P., Ghoniem, A., 2012. Numerical simulation of ion-transport membrane reactors: oxygen permeation and transport and fuel conversion. J. Membr. Sci. 407–408, 71–85.

International Energy Agency, 2008. CO_2 Capture and Storage – A Key Carbon Abatement Option.

Korens, N., Simbeck, D.R., Wilhelm, D.J., 2002. Process screening analysis of alternative gas treating and sulfur removal for gasification , Mountain view, CA, USA.

Kumar, M., Ghoniem, A., 2012. Multi-physics simulations of entrained flow. Part II. Constructing and validating the overall model. Energy Fuels 26, 464–479.

Lozza, G., 1990. Bottoming steam cycles for combined gas-steam power plants: a theoretical estimation of steam turbine performance and cycle analysis. In: ASME Cogen-Turbo, New Orleans.

Macchi, E., Consonni, S., Lozza, G., Chiesa, P., 1995. An assessment of the thermodynamic performance of mixed gas-steam cycles. A. intercooled and steam-injected cycles. J. Eng. Gas Turbines Power Trans. ASME 117, 489–498.

Manzolini, G., Macchi, E., Gazzani, M., 2012. CO_2 capture in natural gas combined cycle with SEWGS. Part B: Economic assessment. Int. J. Greenh. Gas Control 12, 502–509.

Manzolini, G., Macchi, E., Gazzani, M., 2013. CO_2 capture in integrated gasification combined cycle with SEWGS – Part B: economic assessment. Fuel 105, 220–227.

Martinez, I., Grasa, G., Murillo, R., Arias, B., Abanades, J., 2013. Modelling the continuous calcination of $CaCO_3$ in a Ca-looping system. Chem. Eng. J. 215–216, 174–181.

Monaghan, R., Ghoniem, A., 2012. A dynamic reduced order model for simulating entrained flow gasifier. Part 1: Model development and description. Fuel 91, 61–80.

Peters, T., Tucho, W.M., Ramachandran, A., Stange, M., Walmsley, J., Holmestad, R., Borg, A., Bredesen, R., 2009. Thin Pd–23%Ag/stainless steel composite membranes: long-term stability, life-time estimation and post-process characterisation. J. Membr. Sci. 326, 572–581.

Peters, T.A., Kaleta, T., Stange, M., Bredesen, R., 2012. Inhibition of hydrogen transport through a selection of thin Pd-alloy membranes by H_2S: membrane stability and flux recovery in H_2/N_2 and WGS feed mixtures. Catal. Today, 8–19.

PH3/14, I. Report, 2000. Leading options for the capture of CO_2 emissions at power stations.

PH4/33, I. Report, 2004. Improvement in power generation with post-combustion capture of CO_2.

Prins, M., 2012. Personal Communication.

Rao, A., Rubin, E., 2002. A technical economic and environmental assessment of amine-based CO_2 capture technology for power plant greenhouse gas control. Environ. Technol. 36, 4467–4475.

Riberiro, R., Grande, C., Rodrigues, A., 2012. Electrothermal performance of an activated carbon honeycomb monolith. Chem. Eng. Res. Des. 90, 2013–2022.

Rubin, E., 2012. Understanding the pitfalls of CCS cost estimates. Int. J. Greenh. Gas Control 10, 9.

Schell, J., Casas, N., Marx, D., Blom, R., Mazzotti, M., 2013. Comparison of commercial and new adsorbent materials for precombustion CO_2 capture by pressure swing adsorption. In: GHGT-11 Conference Proceedings, Kyoto, 19–23 November 2012.

Schinignitz, M., Tietze, G., 2008. Combined use of carbon dioxide and nitrogen in a component of a powder injection system for use in pulverized coal gasification under pressure.

Scholes, C.A., Smith, K.H., Kentish, S.E., Stevens, G.W., 2010. CO_2 capture from precombustion processes – strategies for membrane gas separation. Int. J. Greenh. Gas Control 4, 739–755.

Song, B., Forsyth, J., 2013. Cachet II: carbon capture and hydrogen production with membranes. Energy Procedia 4, 745.

Valenti, G., Bonalumi, D., Macchi, E., 2012. A parametric investigation of the chilled ammonia process from energy and economic perspectives. Fuel 101, 74–83.

Van Berkel, F., Hao, C., Bao, C., Jiang, C., Xu, H., Morud, J., Peters, T., Soutif, E., Jansen, D., Song, B., 2013. Pd-membranes on their way towards application for CO_2 capture. Energy Procedia 37, 1076.

Wang, M., Lawal, A., Stephenson, P., Sidders, J.C.R., 2011. Post-combustion CO_2 capture with chemical absorption: a state-of-the-art review. Chem. Eng. Res. Des. 89, 1609–1624.

White, V., Torrente-Murciano, L., Sturgeon, D., Chadwick, D., 2010. Purification of oxyfuel-derived CO_2. Int. J. Greenh. Gas Control 4, 137–142.